HHS Public Access

Author manuscript

Nat Med. Author manuscript; available in PMC 2014 December 01.

Published in final edited form as:

Nat Med. 2014 June ; 20(6): 607–615. doi:10.1038/nm.3541.

Tumor Endothelium FasL Establishes a Selective Immune Barrier Promoting Tolerance in Tumors

Gregory T. Motz[1], **Stephen P. Santoro**[1], **Li-Ping Wang**[2], **Tom Garrabrant**[1], **Ricardo R. Lastra**[2], **Ian S. Hagemann**[2], **Priti Lal**[2], **Michael D. Feldman**[2], **Fabian Benencia**[1], and **George Coukos**[1]

[1]Ovarian Cancer Research Center University of Pennsylvania School of Medicine, Philadelphia, PA 19104, USA

[2]Department of Pathology and Laboratory Medicine, University of Pennsylvania, Philadelphia, PA 19104, USA

Abstract

We describe a novel mechanism regulating the tumor endothelial barrier and T cell homing to tumors. Selective expression of the death mediator Fas ligand (FasL/CD95L) was detected in the vasculature of many human and mouse solid tumors but not in normal vasculature, and in these tumors it was associated with scarce $CD8^+$ infiltration and predominance of $FoxP3^+$ T regulatory (Treg) cells. Tumor-derived vascular endothelial growth factor A (VEGF-A), interleukin 10 (IL-10) and prostaglandin E_2 (PGE_2) cooperatively induced FasL expression on endothelial cells, which acquired the ability to kill effector $CD8^+$ T cells, but not Treg cells, due to higher levels of cFLIP expression in Tregs. In the mouse, genetic or pharmacologic suppression of FasL produced a significant increase in the influx of tumor-rejecting $CD8^+$ over $FoxP3^+$ T cells. Pharmacologic inhibition of VEGF and PGE_2 attenuated tumor endothelial FasL expression, produced a significant increase in the influx of tumor-rejecting $CD8^+$ over $FoxP3^+$ T cells, which was FasL-dependent, and led to CD8-dependent tumor growth suppression. Thus, tumor paracrine mechanisms establish a tumor endothelial death barrier, which plays a critical role in establishing immune tolerance and determining the fate of tumors.

Introduction

Engaging the immune system promises to be a critical component of optimal cancer therapy [1]. Despite effective strategies to elicit an immune response, effective tumor control depends in part on the ability of tumor-reactive T cells to infiltrate tumors. Cancer patients with high levels of intratumoral T cells experience significantly increased survival across multiple tumor types [2-6], and experimentally, T cell infiltration is critical for optimal anti-tumor immunity and elimination [7-9]. Tumors exploit complex biological programs linking

Author Contributions: G.T.M. designed experiments, generated data, performed analysis, and wrote the manuscript. S.P.S., T.G., and F.B. generated data. L.W. performed the immunohistochemical staining. R.R.L, I.S.H, P.L., and M.D.F. provided pathology support and scoring assistance. G.C. conceived the project, performed analysis, and co-wrote the manuscript.

angiogenesis and immune evasion [10-11], and tumor angiogenesis is often associated with suppression of T cell-mediated tumor rejection [2,12-13]. The factors driving angiogenesis exert much of their action through the endothelium, and we [14], and others [15], have found that, under their influence, the tumor endothelium establishes a substantial barrier that limits T cell infiltration, which we named the tumor endothelial barrier. Thus, cancer immunotherapy depends on developing strategies to dismantle the tumor endothelial barrier.

To date, the studies investigating the tumor endothelial barrier have focused largely on endothelial-T cell adhesive interactions regulating T cell trafficking. Potent proangiogenic growth factors, including the vascular endothelial growth factor A (VEGF-A), attenuate endothelial-T cell adhesion through deregulation of vascular cell adhesion molecule 1 (VCAM-1) and intercellular adhesion molecule 1 in endothelial cells [16-17]. In addition, the endothelin-endothelin B receptor (ET_BR) pathway, involved in vascular regulation, limits T cell adhesion to endothelium. Experimentally, blockade of VEGF-A [8] or ET_BR [14] increases the amount of T cell infiltration in tumors, and enhances immune therapy. Emerging evidence suggests that the endothelium acts as a selective barrier, allowing certain T cell subsets, notably T regulatory (Treg) cells, to traffic more effectively [18]. However, the above studies have not explored this differential regulatory role of tumor endothelium.

Fas ligand (FasL/CD95L) is an established homeostatic mediator of T cell apoptosis [19] reportedly expressed also on tumor endothelium of humans [20] and mice [21]. Transgenic overexpression of FasL on normal endothelium significantly impairs T cell infiltration in transplant [22] and ischemia-reperfusion injury mouse models [23]. Here, we demonstrate that FasL can be expressed specifically by the vasculature of human solid tumors, and is upregulated by the cooperative action of proangiogenic and immunosuppressive paracrine factors in the tumor microenvironment. In the human, endothelial FasL expression was associated with the absence of intratumoral $CD8^+$ T cells (but not Treg), while in the mouse, endothelial FasL impaired T cell infiltration in tumors in a selective manner, leading to preferential killing of tumor-reactive $CD8^+$ T effector, but not Treg cells, thereby establishing a CD8/FoxP3 T cell ratio that facilitates tumor growth. Pharmacologic inhibition of such factors attenuated tumor endothelial FasL expression, produced a significant increase in $CD8^+$ T cell infiltration, and led to CD8-dependent tumor growth suppression. This work provides new insights into a selective endothelial immune barrier, which establishes immune tolerance in tumors.

Results

The human tumor endothelium expresses FasL

We analyzed expression of FasL in tissue microarrays (TMAs) containing over 600 samples of human breast, colon, renal, bladder, prostate or ovarian adenocarcinomas (Supplementary Table 1) and control TMAs containing normal organs, using well validated antibodies (Supplementary Fig. 1). In agreement with others [20], normal organ vasculature expressed no FasL (Fig. 1a and Supplementary Fig. 2), whereas a substantial percentage of $CD34^+$ blood vessels expressed FasL in primary and metastatic tumors (Fig. 1a, b, c and d, and Supplementary Fig. 3a). In line with previous reports [24], high levels of FasL were detected also in tumor cells of some tumors (Supplementary Fig. 3b–d), but in the majority of tumors,

tumor cells expressed no or low levels of FasL (Fig. 1 and Supplementary Fig. 3c,d). Thus, FasL expression in most tumors is relatively specific to tumor endothelium. Surface FasL expression was verified on freshly isolated $CD45^{-}CD31^{+}$ tumor endothelial cells (TECs) from ovarian cancers (Fig. 1c, d).

We have previously reported an unexplained dichotomy between tumor islets and tumor stroma with respect to T cell infiltration in ovarian cancer: although the vast majority of ovarian cancers exhibit T cell infiltration in the stroma, only a proportion of tumors exhibit T cells infiltrating tumor islets (intraepithelial or intratumoral T cells) [2]. We examined FasL expression in tumor islets and surrounding stroma of ovarian cancer patients. Endothelial FasL expression was significantly higher in tumor islets, while the endothelial cells in the surrounding stroma expressed significantly lower or no FasL (Fig. 1e, f). This suggests a tight regulation of FasL expression in tumors, and implies an important role in regulating T cell homing.

Human endothelial cells expressing FasL kill specifically effector T cells

Because FasL is a known death ligand for activated T cells, we tested whether endothelial cells isolated freshly from tumors can kill activated T cells. We isolated TECs from human ovarian cancer samples and co-incubated them with tumor-associated T lymphocytes (TALs) isolated from autologous ascites, which were previously activated with PMA/ionomycin. We found that TECs killed autologous TALs, which was attenuated by anti-FasL blocking antibody (Fig. 2a).

Because the fate of antitumor immune response depends on the balance between T effector (Teff) and Treg cells in tumors, we asked whether endothelial FasL affects various T cell subsets differently. Immortalized HMEC-1 human endothelial cells were transduced with either GFP or FasL, and incubated with different human T cell subsets purified from peripheral blood of normal donors. As expected, unstimulated T cells were insensitive to killing by $FasL^{+}$ HMEC cells. However, following stimulation with an anti-CD3 antibody and IL-2 for 72 h, both $CD8^{+}$ and $CD4^{+}CD25^{-}$ T cells were sensitized to FasL killing. Importantly, $CD4^{+}CD25^{+}$ cells were largely resistant to FasL killing (Fig. 2b). These results suggest that tumor endothelium FasL plays a critical role in regulating the balance between Teff and Treg cells in tumors.

We then examined the mechanisms of Treg resistance to FasL killing. Compared to $CD8^{+}$ and $CD4^{+}CD25^{-}$ T cells, $CD4^{+}CD25^{+}$ cells expressed higher levels of several anti-apoptotic genes including BCL2, $BCLx_{L}$, and FADD-like IL-1β-converting enzyme-inhibitory protein (c-FLIP) short (c-$FLIP_{S}$) and long (c-$FLIP_{L}$) isoforms (Fig. 2c). Using shRNA, we found that knockdown of c-$FLIP_{S}$ and c-$FLIP_{L}$, but not BCL2 or BCLxL, in Treg enhanced their sensitivity to endothelial FasL (Fig. 2d). *Vice versa*, we found that transduction of $CD8^{+}$ and $CD4^{+}CD25^{-}$ T cells with either c-$FLIP_{S}$ or c-$FLIP_{L}$ increased resistance to FasL-mediated apoptosis, while BCL2 or $BCLx_{L}$ had no effect (Fig. 2e). Thus, c-FLIP mediates FasL resistance in T cells, and enhanced c-FLIP expression is responsible for FasL resistance in Tregs.

We examined human tumors for associations between endothelial FasL and T cell subsets. In an ovarian cancer cohort, where similar to previous observations [2], intraepithelial $CD3^+$ or $CD8^+$ cells were associated with significant increases in overall survival (Supplementary Fig. 4a,b), a high percentage of $FasL^+$ vessels in tumor islets was associated with fewer intraepithelial $CD3^+$ cells (Supplementary Fig. 4c). This difference in $CD3^+$ numbers was largely due to $CD8^+$ cells, since tumors exhibiting a high percentage of $FasL^+$ vessels lacked intraepithelial $CD8^+$ TILs, but exhibited significant intraepithelial $FoxP3^+$ cell numbers (Fig. 2f, g and Supplementary Fig. 4c). Importantly, we found no correlation of intraepithelial $CD8^+$ cell numbers and FasL expression by tumor cells (Supplementary Fig. 4d). We extended these observations to additional tumor types, and found that endothelial, but not tumor cell, FasL expression was associated with fewer $CD8^+$ cells in colon, bladder, prostate, and renal cancers, but not in breast cancer (Fig. 2g and Supplementary Fig. 4e). Thus, tumor endothelium upregulates FasL and acquires the ability to selectively eliminate Teff cells, while allowing accumulation of Treg cells, a phenomenon which appears preserved across several solid tumor types.

Soluble tumor factors cooperate to induce endothelial FasL expression *in vitro*

The compartmentalized expression of endothelial FasL in tumors (Fig. 1e,f) suggests a tight regulation by local factors. To test the hypothesis that paracrine factors produced by tumor cells upregulate endothelial FasL, we treated HMVECs *in vitro* with ovarian cancer ascites, which contains tumor-derived soluble factors. Ascites supernatants were gathered from individuals with ovarian cancer. Approximately half of the supernatants were sufficient to induce FasL in HMVECs *in vitro* (Fig. 3a). We next exposed HMVECs *in vitro* to supernatants of 13 ovarian cancer cell lines maintained under normoxic or hypoxic conditions. Normoxic supernatants of some cell lines were able to induce FasL expression, while supernatants from hypoxic cells induced higher expression of FasL on HMVECs (Fig. 3b,c). Thus, tumor-derived factors (in part hypoxia-related) are responsible for the induction of endothelial FasL.

We screened known tumor-derived factors such as endothelin-1, reactive oxygen species, transforming growth factor-beta (TGF-β), and VEGF-A and found them unable to induce FasL directly in HMVECs (Supplementary Fig. 5 and Fig. 3d). However, interleukin-10 (IL-10) and prostaglandin-E2 (PGE_2) had a direct effect, which was augmented by VEGF-A, and we found significant positive interactions among these three factors (Fig. 3d and Supplementary Fig. 5f,g). We were unable to detect any soluble FasL in the supernatant of treated cells by ELISA (data not shown), in line with the observation that tumor endothelial cells retain FasL on their surface [21]. We next confirmed that treatment with the PGE_2, VEGF-A and IL-10 cocktail was sufficient to enable HVMECs to kill Jurkat T cell targets via FasL *in vitro* (Fig. 3e). Accordingly, we found a positive correlation between the ability of ascites supernatants to induce FasL expression in HMVECs *in vitro* and paucity of intraepithelial TILs in matched ovarian cancer samples *in vivo* (Fig. 3f).

We sought to inhibit induction of FasL through available pharmacologic means. VEGF-A inhibition using an anti-VEGF-A antibody was sufficient to prevent FasL induction by supernatants collected under hypoxic conditions from some, but not all, ovarian cancer cell

lines (Fig. 3g). We used acetylsalicylic acid (ASA) as a means to inhibit cyclooxygenase (COX) 1 and COX2 activity and PGE_2 production. ASA treatment abrogated entirely FasL induction by OV68-4 supernatants, but both ASA and anti-VEGF-A antibody were required to block FasL induction by OVCAR3 supernatants (Fig. 3h). The ability to abrogate FasL induction using a single inhibitor (either anti-VEGF-A or ASA) largely depended on the relative level of COX enzyme expression (Supplementary Fig. 6). High COX1-expressing cell lines were able to induce FasL without VEGF present, and lower expressing lines had an absolute requirement for VEGF-A. Thus, VEGF-A is necessary, but not sufficient for FasL induction on endothelial cells, and paracrine tumor microenvironment factors cooperatively induce FasL on endothelial cells *in vitro*.

COX and VEGF expression regulate endothelial FasL expression *in vivo*

We analyzed VEGF-A, COX1 and COX2 in tumors from individuals with ovarian cancer in order to determine whether a relationship to endothelial FasL expression exists (Fig. 4a). The majority of ovarian cancer samples were negative for COX2, as noted by others [25], and in agreement with our cell line data (Supplementary Fig. 6). COX1 was expressed at high levels by tumor cells, as reported by others [25] (Supplementary Fig. 7a). In our cohort, VEGF-A was highly expressed by tumor cells in the majority of samples (Supplementary Fig. 7a). COX1 expression or co-expression of COX1 and VEGF-A were associated with increased percentage of FasL-positive vessels in tumor islets (Fig. 4b). Furthermore, reanalysis of Affymetrix data from microdissected TECs [14] revealed correlations between endothelial FasL and the expression of PGE_2 as well as VEGF receptors (Supplementary Fig. 7b). Thus, COX1 and VEGF-A are coexpressed and can regulate endothelial FasL expression in human ovarian cancer.

Next, we analyzed these mechanisms *in vivo* using established mouse tumor models, including the ID8-VEGF murine ovarian cancer model [26] as well as models of colon cancer (CT26), renal cell cancer (Renca) and melanoma (B16). ID8-VEGF cells express high levels of Vegf-a and prostaglandin *in vitro* (Supplementary Fig. 8a,b), but express no FasL *in vitro* or *in vivo* (Fig 4c and Supplementary Fig. 8c,d,e). Corroborating our observations in humans, the endothelium of subcutaneous (s.c.) or intraperitoneal (i.p.) ID8-VEGF tumors expressed surface FasL (Fig. 4c–g, and Supplementary Fig. 9a), while FasL was absent from endothelial cells in normal mouse tissues (Supplementary Fig. 9a). Importantly, $CD45^{-}CD31^{+}$ endothelial cells were the predominant FasL expressing cell type in tumors (Supplementary Fig 9b). Although we detected FasL on some $CD45^{+}$ cells (Supplementary Fig 9b), these $FasL^{+}$ cells were rare as determined by IHC (Fig. 4c), and their origin from contaminating peripheral blood cells from the tumor dissociation could not be excluded. Similar data were observed in the other three tumor models (not shown).

Therapeutic administration of the anti-Vegf-a antibody G6-31 combined with ASA reduced the overall number, and percentage, of FasL-positive tumor vessels in all the above tumor models *in vivo* (Fig. 4e and Supplementary Fig. 11d). Use of indomethacin or sulindac sulfide instead of ASA to inhibit Cox enzymes, or blockade of Vegf signaling with SU-5416, also reduced FasL expression (Supplementary Fig. 10b). Vegf-a blockade and Cox inhibition attenuated FasL expression only on tumor endothelial cells, but not on tumor-

infiltrating CD45$^+$ cells (Supplementary Fig. 9b, c), indicating independent regulatory mechanisms. Importantly, Vegf-a blockade and Cox inhibition (ASA) resulted in significant tumor growth suppression in all tumor models *in vivo* (Fig. 4h,i). Thus, like in human solid tumors, mouse tumor endothelium upregulates FasL, which can be attenuated by blockade of Cox plus Vegf-a.

Endothelial FasL preferentially modulates CD8$^+$ cells in mouse tumors

We tested whether tumor endothelial FasL regulates the infiltration of CD8$^+$ T effector (Teff) cells versus Treg cells *in vivo*. Freshly isolated TECs from ID8-VEGF tumors, which express FasL (Fig. 4c,e), killed activated C57BL/6 spleen T cells in a dose-dependent manner *in vitro* (Fig. 5a). Next, we inoculated ID8-VEGF tumors in wild-type (WT), FasL^{gld} (FasL-deficient), Fas^{lpr} (Fas-deficient) mice, or mice treated with an anti-FasL antibody, and found that disruption of Fas-FasL signaling resulted in marked increase in spontaneous CD8$^+$ TILs and in the ratio of CD45$^+$CD3$^+$CD8$^+$ to CD45$^+$CD3$^+$CD4$^+$CD25$^+$FoxP3$^+$ T cells (CD8/Treg) (Fig. 5b and Supplementary Fig. 11a,b). Further, Fas-FasL signaling abrogation resulted in reduced tumor volumes compared to controls (Fig 5c). Thus, disruption of Fas-FasL interactions enhances homing of T cells to tumors and improves the balance between Teff to Treg cells, which affects tumor growth.

Next, we found that pharmacologic inhibition of Vegf-a with G6-31 antibody and Cox enzymes with ASA was sufficient to induce a significant increase in tumor-infiltrating CD8$^+$ T cells, while Tregs remained unaltered in multiple tumor models (Fig. 5d and Supplementary Fig. 10b and 11c). In fact, the frequency of CD8$^+$ cells in tumors was negatively correlated with the number of FasL-positive vessels in these experiments (Fig. 5e and Supplementary Fig. 10d). Corroborating evidence that immune effector mechanisms were activated upon FasL attenuation, we observed a highly oligoclonal T cell receptor (TCR) repertoire of T cells in the tumors of mice treated with an anti-Vegf-a antibody and ASA, with shared TCR sequences among mice, indicating responses to immunodominant tumor epitopes (Fig. 5f). Furthermore, a substantial increase in IL-2, IFN-γ and granzyme-B mRNA expression was seen in tumors of mice treated with anti-Vegf-a antibody and ASA for five weeks (Fig 5g).

Finally, to determine whether FasL ectopically expressed on the endothelium can prevent CD8$^+$ T cell infiltration during anti-Vegf-a and ASA treatment we used a chimeric transplantation model, co-injecting MS1 endothelial cells, transduced (or not) with mouse FasL, and ID8-VEGF tumor cells. This model allows for the development of vessels that are in large developed by exogenous MS1 cells *in vivo* [27-28] (Supplementary Fig. 12). Tumors enriched with control MS1 cells responded to treatment with anti-Vegf-a and ASA, which increased CD45$^+$CD3$^+$CD8$^+$ TILs and resulted in significant tumor suppression (Fig. 5h). In contrast, tumors enriched with MS1 cells with forced expression of FasL were resistant to treatment with anti-Vegf-a and ASA, which did not increase CD45$^+$CD3$^+$CD8$^+$ T cells (Fig. 5h) compared to untreated controls. Therefore, the therapeutic effect of ASA and anti-VEGF-A treatment is mediated by abrogation of endothelial FasL, which enables CD8$^+$ T cell infiltration in tumors.

Cox and Vegf blockade promotes tumor-suppressing immunity

We examined whether the changes in $CD8^+$ infiltrate caused by the combination of anti-Vegf-a antibody and ASA administration was responsible for controlling the growth of tumors. The combined pharmacologic inhibition of Vegf-a and prostaglandin had a strong therapeutic effect on subcutaneous (Fig. 4h,i) as well as intraperitoneal ID8-VEGF tumors (Supplementary Fig. 13a), where it delayed ascites accumulation and significantly prolonged mouse survival. Treatment with indomethacin or sulindac sulfide instead of ASA to inhibit Cox enzymes, or blockade of Vegf signaling with SU-5416 also delayed tumor growth similarly (Supplementary Fig. 10a). The addition of IL-10 blockade did not significantly improve inhibition of tumor growth in this setting (Supplementary Fig. 13b). FasL-positive vessels were positively correlated with tumor volume across all mouse groups ($r = 0.353$, $P = 0.0066$). The expression of FasL on $CD45^+$ cells had no relationship to tumor size in mice (Supplementary Fig. 9e). Suggesting CTL-mediated tumor suppression, CD8 cell density (Fig. 5e and Supplementary Fig. 10e) as well as the levels of IFN-γ and granzyme-B mRNA in tumors (Supplementary Fig. 14) were negatively correlated with tumor volume across all tumor models treated with an anti-Vegf-a antibody and ASA. To test whether the above pharmacologic combination depended on mobilization of antitumor immunity, we depleted $CD8^+$, $CD4^+$ cells, or both subsets. Depletion of $CD8^+$ cells, but not $CD4^+$ cells, abrogated the ability of the anti-Vegf-a antibody and ASA combination to inhibit tumor growth (Fig. 5i,j). Interestingly, 25% (2/8) of mice depleted of $CD4^+$ cells completely eliminated their tumors, and overall $CD4^+$ depletion enhanced anti-tumor immunity, consistent with prior reports indicating that this effect is due to depletion of Tregs [29].

Blockade of FasL enhances T cell infiltration and impairs tumor growth following adoptive transfer

To further test whether endothelial FasL affects the homing of tumor-reactive T cells, we performed adoptive transfer experiments using donor T cells from mice previously vaccinated with a whole tumor lysate vaccine [14]. Tumor-bearing wild-type mice were pretreated with either ASA plus anti-Vegf-a antibody, or with anti-FasL antibody, for 48 hours before receiving donor T cells, followed by 48 hours treatment with the same regimen, and we also used $FasL^{gld}$ tumor-bearing mice as control recipients. Donor T cells were purified from splenocytes of vaccinated mice, labeled with CFSE, and transferred into recipient mice, which were not irradiated to avoid endothelial activation [30]. We found that vaccine-primed $CD8^+$ T cells infiltrated tumors to a higher degree in the two treatment groups and in $FasL^{gld}$ mice compared to untreated wild-type controls (Fig. 6a,b, and c). Importantly, there was a higher frequency of apoptotic T cells (annexin-V^+ $CFSE^+$ $CD8^+$ cells) isolated from dissociated tumors of control mice compared to treatment groups or $FasL^{gld}$ mice (Fig. 6d). In spite of these obvious differences in tumor-infiltrating T cells, we detected no difference in T cell homing or survival in spleens between control and treated mice (data not shown), with the exception of marginally increased survival of spleen T cells in $FasL^{gld}$ recipient mice.

To determine whether the observed enhanced T cell homing and survival observed under conditions of inhibiting FasL could impact mouse survival, we performed adoptive transfer experiments using activated OT-1 cells in mice inoculated with OVA-expressing ID8-VEGF

cells (Fig. 6e). We found that adoptive transfer of activated OT-1 cells in FasL^{gld} mice or in wild-type mice pretreated with ASA plus anti-Vegf-a significantly prolonged survival when compared to controls. Thus, inhibiting endothelial FasL expression is a robust therapeutic maneuver enhancing the potency of adoptive transfer of anti-tumor T cells.

Discussion

An emerging paradigm supported by our recent work [10-11] is that angiogenesis and immune suppression are two facets of a linked biological program. Tumors co-opt existing mechanisms that are normally required to limit excessive inflammation and promote tissue recovery during infection or wound healing, and the execution of this program sustains tumor growth and promotes immunological tolerance. The tumor endothelium is a prime example of this concept, and existing work has largely focused on the angiogenic tumor endothelium as a physical passive barrier, preventing T cell extravasation and effective anti-tumor immunity through anergy [8,10,14]. However, new evidence suggests the tumor endothelium is also an active immune regulator that can directly suppress T cell function [31]. Our current work expands this hypothesis with the demonstration that angiogenic growth factors induce FasL expression on the tumor endothelium, which uniquely promotes an immunosuppressive and tolerogenic environment through preferential killing of tumor-reactive CD8$^+$ cells.

FasL has an extensive history as a mediator of immune privilege, albeit controversial, particularly in the context of tumor biology [32]. Chemical alteration [33] and cellular location of expression (i.e., membrane or soluble) [34] can significantly impact the biological activity of FasL. Membrane expression of FasL is highly cytotoxic [34], whereas soluble FasL may only exert full cytotoxicity in oxygen rich environments [33]. In the current study, we found tumor cell expression of FasL by IHC, but were unable to detect surface expression on EpCAM$^+$ tumor cells by flow cytometry (not shown). Further, a panel of ovarian cancer cell lines did not express surface FasL (not shown). This observation recapitulates several reports noting a lack of surface expression of FasL by tumors and tumor cell lines [35-36], and although it has been suggested that FasL-containing exosomes may contribute to T cell apoptosis and immune privilege [36], the importance of this mechanism *in vivo* is unknown. We observed a strong inverse association between vessel FasL expression and CD8$^+$ TILs, but we observed no relationship across multiple tumor types with respect to CD8$^+$ TILs and expression of FasL by tumor cells. This observation is not without precedent [37-38], and we attribute this phenomenon to greater cytotoxicity of membrane-expressed FasL on the tumor endothelium in both patients and mice.

Numerous investigators have noted that during immunotherapy, anti-tumor T cells could be found in abundance in the periphery, but that often these cells failed to penetrate the tumor in large numbers [39-41]. Enhanced tumor angiogenesis is commonly associated with absence of tumor-infiltrating T cells in patients [2,12], and multiple investigators have determined that inhibition of angiogenesis promotes infiltration of anti-tumor T cells during adoptive therapy [8,14,42]. Mechanistically, existing data indicates that angiogenesis can reduce endothelial adhesion and migration of T cells [16-17,43]. In agreement with others, overall intratumoral T cell numbers were increased following angiogenesis blockade, but this was

largely restricted to $CD8^+$ T cells, as $FoxP3^+$ cell numbers remained unchanged. Further, in mice that were either deficient in Fas-FasL signaling, or treated with an anti-FasL antibody, intratumoral $CD8^+$ T cell numbers were increased and tumor volumes were decreased independently of any effect on angiogenesis. Thus, we conclude that blocking tumor angiogenesis primarily promotes effector $CD8^+$ T cell infiltration by limiting effector T cell apoptosis mediated by FasL expression on the tumor endothelium. These observations are particularly relevant for *ex vivo* activated T cells used for adoptive cell therapy, as well as endogenous T cells activated in lymph nodes by cancer vaccines, as post-activation T cells are highly susceptible to FasL-mediated apoptosis.

VEGF-A and prostaglandins exert immunosuppression through diverse mechanisms [10], so it is not surprising that treatment with anti-VEGF-A antibody and aspirin enhanced antitumor immunity. The finding, supported by others [42], that angiogenesis blockade required $CD8^+$ T cells supports the notion that factors like VEGF-A do not simply promote tumor growth through angiogenesis. Importantly, although anti-VEGF-A antibody and aspirin could inhibit angiogenesis directly, effective tumor control remained dependent on an anti-tumor T cell response. Furthermore, we found that when FasL was ectopically expressed on the endothelium, it prevented infiltration of $CD8^+$ T cells and prevented decreases in tumor growth despite effective treatment with angiogenesis inhibitors. Therefore, the roles of VEGF-A and COX1 in promoting tumor growth are not solely mediated by their classical roles in angiogenesis and rather extend to vascular mechanisms controlling mobilization of antitumor immunity.

The regulation of FasL expression by the endothelium is complex, and the integration of multiple tumor microenvironment growth factors leads to optimal FasL expression by the endothelium. Therefore, although VEGF-A or PGE2 alone are not sufficient for endothelial FasL expression, each is required. Thus, inhibition of FasL expression using single blockade (either inhibition of VEGF-A or COX) can be observed (Fig. 4e). Therapeutically, identification of the signaling pathway in endothelial cells that is responsible would allow for optimal disruption of FasL expression with a single reagent, and is being actively pursued.

Immunotherapy or anti-angiogenesis therapy have often been pursued as monotherapies. We have shown here how adoptive T cell transfer combined with aspirin and an anti-VEGF-A antibody led to superior infiltration of tumor-reactive T cells. This combinatorial approach is supported by previous work showing enhanced control of tumor growth using a tumour lysate vaccine and ET_BR blockade [14], a tumor lysate-pulsed DC vaccine with COX2 inhibitors [44], or adoptive T cell therapy with VEGF-A-specific neutralizing antibody [8]. Further, similar additive benefits were observed in patients by combining recombinant IFN-α therapy and bevacizumab for the treatment of metastatic renal cell carcinoma [45]. Therefore, because of the intimate relationship between angiogenesis and immunosuppression and the likely overwhelming redundancy of pathways controlling both mechanisms, combinatorial strategies inhibiting both arms will be required for effective tumor control.

Methods

Mice

C57BL/6J, B6Smn.C3-*Fasl*^{gld}/J, B6.MRL-*Fas*^{lpr}/J, BALB/cJ, and NU/J mice were obtained from the Jackson Laboratory. All mice used were female, aged 8–10 weeks. All of the experimental protocols were reviewed and approved by the Institutional Animal Care and Use Committee at the University of Pennsylvania.

Isolation of clinical samples for flow cytometry. Ovarian tumors were obtained from individuals undergoing primary resection and were used for processing

For T cell staining, tumor samples were minced finely with a razor blade, followed by overnight room-temperature enzymatic digestion with collagenase and DNase in serum-free RPMI. Digested tumors were then processed through a cell homogenizer sieve (Bellco), followed by red blood cell lysis and additional passage through a 100 μM cell strainer. Cell suspensions were then placed over a Ficoll gradient to remove dead cells and debris, and cells collected at the interphase were used for FACS analysis. Enzymatic digestion was found to significantly reduce the ability to detect surface FasL expression, and this step was omitted for samples stained for FasL. Ascites was drawn aseptically during surgical procedures, and cleared by centrifugation followed by storage of the resultant supernatants at −80 °C until used. All human specimens were processed in compliance with the institutional review board at the University of Pennsylvania and the US Health Insurance Portability and Accountability Act (HIPAA) requirements.

Human tumor microarray

Tissue microarrays was developed by the University of Pennsylvania Tissue Microarray Facility in the Department of Pathology using a series of breast (n = 62), colon (n = 17), renal (n = 95), bladder (n = 203), prostate cancers (n = 25) and ovarian (207 primary and metastatic tumor samples from 53 ovarian cancer patients with treatment-naive stage II-IV papillary serous epithelial ovarian cancer). Patients underwent resection at the Hospital of the University of Pennsylvania between 2005 and 2008. Slides stained with hematoxylin and eosin were reviewed and annotated by a trained pathologist, and paraffin-embedded tissue blocks were selected to construct a tissue microarray. For each sample, triplicate 0.6mm cores of tumor at five micron thickness were placed on a tissue microarray using a manual arrayer. This tissue microarray was used for all immunohistochemical staining, and scoring of immunohistochemical staining was performed by two observers in a blinded manner. Similar methodologies were applied to arrays from additional tumor types. All human specimens were processed in compliance with the institutional review board at the University of Pennsylvania and the US Health Insurance Portability and Accountability Act (HIPAA) requirements.

Growth of cell lines

HMVEC cells (Lonza) were expanded and used from passage 3–7. Endothelial cells were grown using EGM-2MV media (Lonza) on cell culture plates coated with 0.2% gelatin. HMEC-1 cells, an SV40 transformed human microvascular endothelial cell line [46], were

obtained from the Centers for Disease Control and Prevention (Atlanta, GA) and grown in MCDB 131 media (Invitrogen) containing mouse EGF (BD), hydrocortisone (Sigma), 10% FBS, 1% PenStrep and 1× GlutaMax (Invitrogen). Ovarian cancer cell lines were obtained from either from ATCC or were a gift from the laboratory of Carl June developed from primary ovarian tumors. All lines were grown in RPMI containing 10% FBS and 1% PenStrep.

Treatment of endothelial cells

For all treatments, 75k cells endothelial cells were plated to gelatin-coated 12 well plates. 24 h later the endothelial cells were washed twice with 1×PBS, and placed in a low-serum media composed of basal EBM-2 endothelial cell media (Lonza) containing 0.5% FBS for 16 h before treatment as indicated in figure legends. For treatment with cell culture supernatants, ovarian cancer cells were grown to sub-confluence, and placed in normoxia or hypoxia (1.5% O_2) for 24 h. Cell culture supernatants were cleared by centrifugation and mixed with low-serum EBM-2 at a 1:1 ratio and placed on endothelial cells for 24 h. For VEGF-A neutralization, 5 μg mL^{-1} anti-VEGF-A antibody (R&D) or isotype was added to cell culture supernatants for 30min at room temperature prior to addition to HMVEC cells. In cases of Aspirin treatment, 200 μM Aspirin was added to cells during exposure to normoxia or hypoxia. For treatments with ascites, samples were mixed with low-serum EBM-2 at a 1:1 ratio and placed on endothelial cells for 24 h. To enhance surface expression of FasL for flow cytometry, a broad spectrum metalloproteinase inhibitor (MMP Inhibitor II, 50nM, EMD Millipore) was added concurrently. For flow cytometry, HMVECs were washed twice with 1× PBS following treatment and detached with 1×PBS containing 2 mM EDTA at 37C for 5-10 min.

Western Blot

HMVECs were treated as indicated, and whole cells lysates were prepared using 1×RIPA buffer containing a protease inhibitor cocktail (Pierce). Equal concentrations (20–25 μg) were loaded following a BCA assay, and were run out on a precast 4–15% SDS-PAGE gradient gel (BioRad). FasL was detected using a polyclonal affinity adsorbed antibody (Cell Signaling) and specificity was confirmed using FasL transfected HEK293 cells. Blots were stripped and reprobed with a monoclonal anti-actin antibody (Sigma). Semi-quantitative densitometry was performed using NIH Image J software.

Growth of Tumors

For ID8-VEGF tumors i.p. and s.c. tumor inoculations, 5×10^6 cells[26] were injected. For additional models, 1×10^6 CT26, 1×10^6 Renca, and 1×10^5 B16-LU8 cells were injected s.c. The development of s.c. tumors were measured with Vernier calipers and tumor volumes were calculated using the equation $V = ½ (L \times W^2)$. The development of i.p. tumors were monitored by the development of ascites, determined by weight. Survival time points were based on a weight of 32g in accordance with IACUC protocols.

Antibody and Aspirin Treatments

For long-term experiments, one day after ID8-VEGF tumor inoculation, mice were injected weekly with 40 μg anti-VEGF-A antibody (~2 mg kg^{-1}; clone G6-31; gift of Genentech), given daily gavage with 2 mg aspirin (~100 mg kg^{-1}; Cayman Chemical), or treated with both interventions. Control mice were given equal amounts of mouse IgG. For long-term experiments with anti-FasL antibody (clone MFL3), mice were given three 25 μg intratumoral injections a week.

T cell depletion

Anti-CD4 (GK1.5) and anti-CD8 (53-6.7) depletion antibodies were harvested from the ascites of NU/J mice injected with the corresponding hybridoma cell lines. Ascites was filtered and antibody concentrations were titered by ELISA. For two days immediately following ID8-VEGF tumor inoculation mice were given 100 μg of the corresponding depletion antibody, and subsequently mice were injected twice weekly with 100 μg of the corresponding depletion antibody. Depletion was confirmed by flow cytometry using alternative antibody clones. Splenocytes from mice were harvested and used for ELISpot analysis using ID8-VEGF cells at a 20:1 splenocyte:tumor cell ratio incubated for 24 h. Specific spots were calculated by subtracting spots from unstimulated wells.

Flow Cytometry

Single cell suspensions were prepared as indicated. For FasL staining of human and mouse endothelial cells from tumor samples, a 3-step staining approach was utilized. Following an initial blocking step, cells were incubated with an unconjugated anti-FasL antibody (NOK-1, human; MFL3, mouse; confirmation of antibody specificity Supplementary Fig. 1), followed by extensive washing. Cells were then stained with the appropriate biotinylated secondary antibody followed by washing and incubation with APC conjugated streptavidin with anti-CD45 (Hl30, human; 30-F11, mouse) and anti-CD31 (WM59, human; 390, mouse). FMO staining using the appropriate isotypes in place of FasL was performed as a control for each sample. Only live ($7AAD^{-}$) singlets were used for all analyses. Mouse Treg analysis was performed using anti-CD3 (145-2C11), anti-CD8 (53-6.7), anti-CD4 (GK1.5), anti-CD25 (PC61), and anti-Foxp3 (FJK-16s).

Immunohistochemistry

For human TMA staining, paraffin-embedded tissues were baked at 60 °C for 1 h, deparrafinized in xylenes, rehydrated in sequential gradations of alcohol, and washed in water. Antigen retrieval was performed using with either citrate or EDTA buffer, depending on the antibody. Endogenous peroxidase was inactivated with Dual Endogenous Enzyme block (Dako). Following antibody incubations, visualization was performed with diaminobenzidine tetrahydrochloride (Dako) or using an alkaline phosphatase red substrate kit (for dual stains). Sections were counterstained with hematoxylin. The following antibodies were used for IHC: anti-human FasL (clone G247-4, BD; confirmation of antibody specificity Supplementary Fig. 1), anti-human CD34 (rabbit polyclonal, Thermo Scientific), anti-human VEGF-A (RB-9031, Thermo Scientific), anti-human COX1 (Clone CX111, Cayman), anti-human COX2 (clone CX-294, Dako), anti-human IL-10 (goat

polyclonal, R&D), anti-human CD8 (clone), and anti-human FoxP3 (clone). Mouse tumors were frozen in OCT, and sectioned at 7 μm thickness, fixed in methanol, and stained and visualized in a similar manner as above. Antibodies used were anti-mouse FasL (N-20, santa cruz; confirmation of antibody specificity Supplementary Fig. 1), anti-mouse CD31 (clone MEC 13.3, BD), anti-mouse CD8 (clone 53-6.7, BD), anti-mouse FoxP3 (clone FJK-16s, eBio). All samples were scanned, and analyzed using ImageScope software.

Generation of FasL transduced HMEC-1 cells

The expression vector pEFBOS-FasL containing the cDNA of human FasL was used to subclone FasL into the lentiviral vector pELNS containing EF1 alpha promoter. Lentivirus was generated as previously published [47]. eGFP or FasL lentivirus was concentrated by ultracentrifugation and used to transduce HMEC-1 cells for experimentation. Expression of eGFP and FasL was determined by flow cytometry.

Generation of transduced T cells

We subcloned human BCL2 and BCLxL using plasmids from available from Addgene. We subcloned cFLIPlong and cFLIPshort using a synthesized plasmid from GeneArt. All genes were subcloned into the lentiviral transduction vector pELNS, and virus was prepared as above. For transduction using shRNA, we used MISSION shRNA (Sigma) plasmids to generate lentivirus. Normal donor T cells were transduced with lentiviral particles following 24 h activation with CD3/CD28 beads using 8 μg mL^{-1} polybrene with spinoculation.

Killing Assays

HMVEC cells were treated with PGE2, VEGF-A, and IL-10 for 24 h as indicated above. HMVEC cells were then washed three times with 1× PBS, and fixed with 2% paraformaldehyde at 4°C for 30min. Fixed endothelial cells were then washed four times with 1× PBS, and Jurkat (E6-1) cells were added at a 3:1 endothelial:Jurkat ratio for 24 h. Where anti-FasL blocking antibody (10 μg mL^{-1}, clone NOK-1) or isotype was used, HMVEC cells were incubated with the antibody for 30 min at 37°C prior to addition of Jurkats. For anti-Fas blocking antibody (1 μg mL−1, clone ZB4) or isotype, Jurkat cells were incubated with antibody 30 min at 37°C prior to addition of cells. Cell death of Jurkats was assessed by flow cytometry using apoptosis detection kit (BD biosciences) that stains for Annexin V and 7AAD.

For assays using normal donor T cells, $CD4^+$ and $CD8^+$ T cell subsets were obtained from the University of Pennsylvania Human Immunology Core. $CD4^+$ T cells were further subdivided into $CD4^+CD25^+$ (>90%) and $CD4^+CD25^-$ (>98%) subsets using $CD25^+$ positive selection beads (Invitrogen). T cells were activated with 2.5 μg mL^{-1} platebound anti-CD3 (OKT3) antibody and IL-2 as previously published [48]. 72 h following activation, T cell subsets were incubated with either GFP or FasL transduced HMEC-1 cells at a 1:1 ratio for 18 h, and T cell viability was determined by flow cytometry using an apoptosis detection kit (BD). Lentiviral transduced T cells were activated during transduction as described above, and were incubated with HMEC-1 cells 96 h after activation.

For assays with *ex vivo* human and mouse tumor endothelial cells, $CD31^+$ cells were isolated from tumor digests by positive selection (Miltenyi) following depletion of $CD45^+$ cells. Autologous human T cells from ascites and mouse splenic T cells were isolated by positive selection (Miltenyi) and activated with PMA/ionomycin. T cell subsets were incubated with isolated endothelial cells at a 1:1 ratio for 18 h, and T cell viability was determined by flow cytometry using an apoptosis detection kit (BD).

PCR

RNA was isolated from tumors or T cells lines using TRIZOL (Invitrogen). RNA was converted to cDNA using the cDNA archive kit (ABI). For qRT-PCR, reactions were carried out using Taqman probes from ABI using the 2× Taqman master mix, following the manufacturer's protocols. All samples were normalized using 18S endogenous control primers.

Spectratyping

cDNA from mouse tumors and spleens was isolated as above. PCR reactions were carried out using previously published [49]. PCR reactions were run on a precast, nondenaturing 10% acrylamide gel (BioRad), followed by visualization with SYBR safe (BioRad), and images were captured with a BioRad Gel Documentation system.

MS1 model

Mouse endothelial MS1 cells (ATCC) were transduced with a lentiviral expression vector for mouse FasL, subcloned from an expression plasmid (gift from Dr. Shigekazu Nagata). 1×10^6 Control, or FasL transduced cells were injected i.t. into 3 wk ID8-VEGF tumors, followed by an additional i.t. injection at 4 wks. Treatments with ASA and anti-VEGF-A were carried out as for long term experiments as indicated above following injection with MS1 cells.

Adoptive Transfer

Donor mice were vaccinated three times with 1×10^7 UVB killed ID8-VEGF cells injected s.c. weekly as previously described [14]. Splenocytes were isolated one week following the last vaccination, and CD8 T cells were isolated by negative selection. T cells were activated with anti-CD3/anti-CD28 Dynal beads (Invitrogen) with 100U mL^{-1} msIL-2 for 96 h. Following activation, T cells were labeled with 10uM CFSE and $9\text{-}10\times10^6$ T cells were injected into recipient mice bearing tumors ~200 mm^3 in size. Prior to injection, mice were treated once daily with either 50 μg anti-FasL (MFL3) antibody or 50 μg anti-VEGF-A and 2 mg Aspirin for 48 h prior to T cell injection. Following T cell injection, mice received the same antibody injections daily for an additional 48 h, followed by harvest at 72 h post T cell injection. Tumors were isolated from recipient mice and processed for flow cytometry as indicated above. For fluorescence imaging, a small section of tumor was frozen in OCT and sectioned at 7 μm. Slides were fixed in acetone and stained with DAPI. For OT-1 adoptive transfer experiments, mice bearing 3 wk ID8-VEGF OVA i.p. tumors were treated as indicated above and then received 3×10^6 peptide activated OT-1 cells i.p.

Statistics

All values are expressed as the mean ± s.e.m. Statistical differences were determined significant *at* $P < 0.05$. Specific tests used are described in the figure legends. All analyses were performed using SigmaPlot Software.

Supplementary Material

Refer to Web version on PubMed Central for supplementary material.

Acknowledgments

This project was supported by US National Institutes of Health Transformative R01 CA156695 (GC), US National Cancer Institute (NCI) training grant T32 CA009140 (GTM), a grant by the Ovarian Cancer Research Fund (GTM), and NCI training grant R25 CA101871 (SPS). We kindly thank S. Nagata (Kyoto University) for the FasL expression plasmids, and C. June (University of Pennsylvania) for the lentivirus expression vector. The authors also thank D. Powell and A. Facciabene for thoughtful discussion.

References

1. Mellman I, Coukos G, Dranoff G. Cancer immunotherapy comes of age. Nature. 2011; 480:480–9. [PubMed: 22193102]
2. Zhang L, et al. Intratumoral T cells, recurrence, and survival in epithelial ovarian cancer. N Engl J Med. 2003; 348:203–13. [PubMed: 12529460]
3. Sato E, et al. Intraepithelial CD8+ tumor-infiltrating lymphocytes and a high CD8+/regulatory T cell ratio are associated with favorable prognosis in ovarian cancer. Proc Natl Acad Sci U S A. 2005; 102:18538–43. [PubMed: 16344461]
4. Hwang WT, Adams SF, Tahirovic E, Hagemann IS, Coukos G. Prognostic significance of tumor-infiltrating T cells in ovarian cancer: a meta-analysis. Gynecol Oncol. 2012; 124:192–8. [PubMed: 22040834]
5. Cipponi A, Wieers G, van Baren N, Coulie PG. Tumor-infiltrating lymphocytes: apparently good for melanoma patients. But why? Cancer Immunol Immunother. 2011; 60:1153–60. [PubMed: 21553145]
6. Galon J, et al. Type, density, and location of immune cells within human colorectal tumors predict clinical outcome. Science. 2006; 313:1960–4. [PubMed: 17008531]
7. Boissonnas A, Fetler L, Zeelenberg IS, Hugues S, Amigorena S. In vivo imaging of cytotoxic T cell infiltration and elimination of a solid tumor. J Exp Med. 2007; 204:345–56. [PubMed: 17261634]
8. Shrimali RK, et al. Antiangiogenic agents can increase lymphocyte infiltration into tumor and enhance the effectiveness of adoptive immunotherapy of cancer. Cancer Res. 2010; 70:6171–80. [PubMed: 20631075]
9. Molon B, et al. Chemokine nitration prevents intratumoral infiltration of antigen-specific T cells. J Exp Med. 2011; 208:1949–62. [PubMed: 21930770]
10. Motz GT, Coukos G. The parallel lives of angiogenesis and immunosuppression: cancer and other tales. Nat Rev Immunol. 2011; 11:702–11. [PubMed: 21941296]
11. Facciabene A, et al. Tumour hypoxia promotes tolerance and angiogenesis via CCL28 and T(reg) cells. Nature. 2011; 475:226–30. [PubMed: 21753853]
12. Bouma-ter Steege JC, et al. Angiogenic profile of breast carcinoma determines leukocyte infiltration. Clin Cancer Res. 2004; 10:7171–8. [PubMed: 15534089]
13. Hamzah J, et al. Vascular normalization in Rgs5-deficient tumours promotes immune destruction. Nature. 2008; 453:410–4. [PubMed: 18418378]
14. Buckanovich RJ, et al. Endothelin B receptor mediates the endothelial barrier to T cell homing to tumors and disables immune therapy. Nat Med. 2008; 14:28–36. [PubMed: 18157142]

15. Quezada SA, et al. Limited tumor infiltration by activated T effector cells restricts the therapeutic activity of regulatory T cell depletion against established melanoma. J Exp Med. 2008; 205:2125–38. [PubMed: 18725522]
16. Bouzin C, Brouet A, De Vriese J, Dewever J, Feron O. Effects of vascular endothelial growth factor on the lymphocyte-endothelium interactions: identification of caveolin-1 and nitric oxide as control points of endothelial cell anergy. J Immunol. 2007; 178:1505–11. [PubMed: 17237399]
17. Griffioen AW, Damen CA, Martinotti S, Blijham GH, Groenewegen G. Endothelial intercellular adhesion molecule-1 expression is suppressed in human malignancies: the role of angiogenic factors. Cancer Res. 1996; 56:1111–17. [PubMed: 8640769]
18. Shetty S, et al. Common lymphatic endothelial and vascular endothelial receptor-1 mediates the transmigration of regulatory T cells across human hepatic sinusoidal endothelium. J Immunol. 2011; 186:4147–55. [PubMed: 21368224]
19. Strasser A, Jost PJ, Nagata S. The many roles of FAS receptor signaling in the immune system. Immunity. 2009; 30:180–92. [PubMed: 19239902]
20. Yu JS, et al. Intratumoral T cell subset ratios and Fas ligand expression on brain tumor endothelium. J Neurooncol. 2003; 64:55–61. [PubMed: 12952286]
21. Bajou K, et al. Plasminogen activator inhibitor-1 protects endothelial cells from FasL-mediated apoptosis. Cancer Cell. 2008; 14:324–34. [PubMed: 18835034]
22. Sata M, Luo Z, Walsh K. Fas ligand overexpression on allograft endothelium inhibits inflammatory cell infiltration and transplant-associated intimal hyperplasia. J Immunol. 2001; 166:6964–71. [PubMed: 11359858]
23. Yang J, et al. Endothelial cell overexpression of fas ligand attenuates ischemia-reperfusion injury in the heart. J Biol Chem. 2003; 278:15185–91. [PubMed: 12576484]
24. Abrahams VM, et al. Epithelial ovarian cancer cells secrete functional Fas ligand. Cancer Res. 2003; 63:5573–81. [PubMed: 14500397]
25. Gupta RA, et al. Cyclooxygenase-1 is overexpressed and promotes angiogenic growth factor production in ovarian cancer. Cancer Res. 2003; 63:906–11. [PubMed: 12615701]
26. Zhang L, et al. Generation of a syngeneic mouse model to study the effects of vascular endothelial growth factor in ovarian carcinoma. Am J Pathol. 2002; 161:2295–309. [PubMed: 12466143]
27. Lam CT, et al. Brain-derived neurotrophic factor promotes tumorigenesis via induction of neovascularization: implication in hepatocellular carcinoma. Clin Cancer Res. 2011; 17:3123–33. [PubMed: 21421859]
28. Tei K, et al. Roles of cell adhesion molecules in tumor angiogenesis induced by cotransplantation of cancer and endothelial cells to nude rats. Cancer Res. 2002; 62:6289–96. [PubMed: 12414659]
29. Turk MJ, et al. Concomitant tumor immunity to a poorly immunogenic melanoma is prevented by regulatory T cells. J Exp Med. 2004; 200:771–82. [PubMed: 15381730]
30. Gaugler MH. A unifying system: does the vascular endothelium have a role to play in multi-organ failure following radiation exposure? BJR Suppl. 2005; 27:100–5.
31. Huang X, et al. Lymphoma endothelium preferentially expresses Tim-3 and facilitates the progression of lymphoma by mediating immune evasion. J Exp Med. 2010
32. Restifo NP. Not so Fas: Re-evaluating the mechanisms of immune privilege and tumor escape. Nat Med. 2000; 6:493–5. [PubMed: 10802692]
33. Herrero R, et al. The biological activity of FasL in human and mouse lungs is determined by the structure of its stalk region. J Clin Invest. 2011; 121:1174–90. [PubMed: 21285513]
34. Suda T, Hashimoto H, Tanaka M, Ochi T, Nagata S. Membrane Fas ligand kills human peripheral blood T lymphocytes, and soluble Fas ligand blocks the killing. J Exp Med. 1997; 186:2045–50. [PubMed: 9396774]
35. Chappell DB, Zaks TZ, Rosenberg SA, Restifo NP. Human melanoma cells do not express Fas (Apo-1/CD95) ligand. Cancer Res. 1999; 59:59–62. [PubMed: 9892185]
36. Andreola G, et al. Induction of lymphocyte apoptosis by tumor cell secretion of FasL-bearing microvesicles. J Exp Med. 2002; 195:1303–16. [PubMed: 12021310]

37. Favre-Felix N, et al. Cutting edge: the tumor counterattack hypothesis revisited: colon cancer cells do not induce T cell apoptosis via the Fas (CD95, APO-1) pathway. J Immunol. 2000; 164:5023–7. [PubMed: 10799856]
38. Donskov F, et al. Fas ligand expression in metastatic renal cell carcinoma during interleukin-2 based immunotherapy: no in vivo effect of Fas ligand tumor counterattack. Clin Cancer Res. 2004; 10:7911–6. [PubMed: 15585624]
39. Lurquin C, et al. Contrasting frequencies of antitumor and anti-vaccine T cells in metastases of a melanoma patient vaccinated with a MAGE tumor antigen. J Exp Med. 2005; 201:249–57. [PubMed: 15657294]
40. Boon T, Coulie PG, Van den Eynde BJ, van der Bruggen P. Human T cell responses against melanoma. Annu Rev Immunol. 2006; 24:175–208. [PubMed: 16551247]
41. Dudley ME, et al. Cancer regression and autoimmunity in patients after clonal repopulation with antitumor lymphocytes. Science. 2002; 298:850–4. [PubMed: 12242449]
42. Manning EA, et al. A vascular endothelial growth factor receptor-2 inhibitor enhances antitumor immunity through an immune-based mechanism. Clin Cancer Res. 2007; 13:3951–9. [PubMed: 17606729]
43. Griffioen AW, Damen CA, Blijham GH, Groenewegen G. Tumor angiogenesis is accompanied by a decreased inflammatory response of tumor-associated endothelium. Blood. 1996; 88:667–73. [PubMed: 8695814]
44. Basu GD, et al. Cyclooxygenase-2 inhibitor enhances the efficacy of a breast cancer vaccine: role of IDO. J Immunol. 2006; 177:2391–402. [PubMed: 16888001]
45. Rini BI, et al. Phase III trial of bevacizumab plus interferon alfa versus interferon alfa monotherapy in patients with metastatic renal cell carcinoma: final results of CALGB 90206. J Clin Oncol. 2010; 28:2137–43. [PubMed: 20368558]
46. Ades EW, et al. HMEC-1: establishment of an immortalized human microvascular endothelial cell line. J Invest Dermatol. 1992; 99:683–90. [PubMed: 1361507]
47. Dull T, et al. A third-generation lentivirus vector with a conditional packaging system. J Virol. 1998; 72:8463–71. [PubMed: 9765382]
48. Strauss L, Bergmann C, Whiteside TL. Human circulating CD4+CD25highFoxp3+ regulatory T cells kill autologous CD8+ but not CD4+ responder cells by Fas-mediated apoptosis. J Immunol. 2009; 182:1469–80. [PubMed: 19155494]
49. Motz GT, et al. Persistence of lung CD8 T cell oligoclonal expansions upon smoking cessation in a mouse model of cigarette smoke-induced emphysema. J Immunol. 2008; 181:8036–43. [PubMed: 19017996]

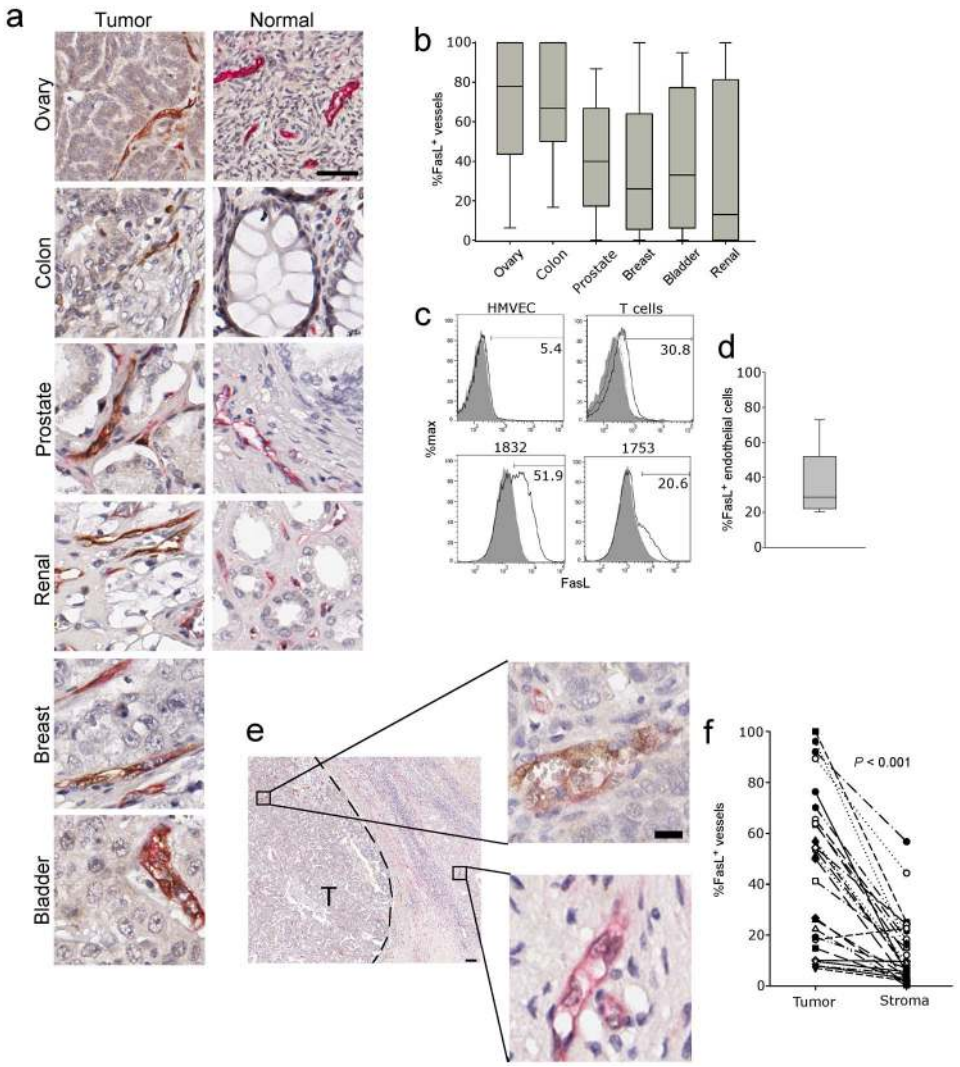

Figure 1. Expression of FasL on the human tumor endothelium

(**a**) Representative dual staining of the endothelium (CD34, Red) and FasL (brown) from normal and tumor tissues from the indicated organs. Original magnification, 400×; scale bar, 50 μm. (**b**) Summary of FasL vessel expression of the indicated tumor types. (**c**) Expression of FasL on cultured normal endothelial cells, activated T cells and two representative ovarian tumor samples gated on $CD45^{-}CD31^{+}$ endothelial cells. Shaded areas are isotype control staining, and dotted line in T cell plot is FasL from unstimulated T cells. All solid lines are FasL staining. (**d**) Quantification of FasL on tumor endothelial cells isolated from individuals with ovarian cancer ($n = 11$). (**e**) Representative image showing vessels from tumor (T) and surrounding stromal tissue. Original magnification 40×; scale bar, 100 μm. Enlarged vessels original magnification 200×; scale bar, 50 μm. (f) Quantification of FasL expression on the tumor endothelium of individuals with ovarian cancer. (n = 27). *P* value determined by a paired t test.

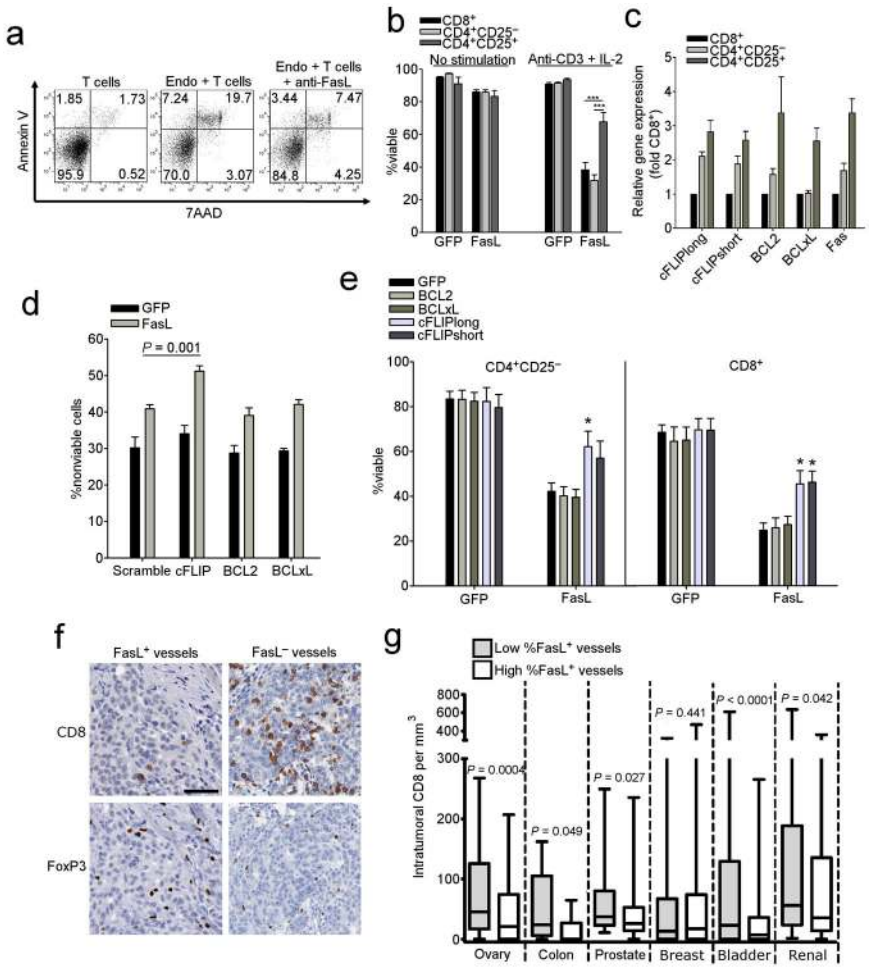

Figure 2. Endothelial FasL kills T cells

(**a**) Viability of T cells following co-culture with endothelial cells isolated from human ovarian tumors incubated at a 3:1 ratio with or without anti-FasL antibody. Gated on $CD3^+$ T cells. (**b**) Killing of normal donor T cell subsets by HMEC-1 cells transduced with either GFP or FasL. Data are means ±SEM pooled from three independent experiments using unique healthy donors. ***$P < 0.001$, values determined by Student's t test. (**c**) Expression of anti-apoptotic genes in human T cell subsets as determined by qRT-PCR. Data are means ±SEM pooled from six independent experiments using unique healthy donors. (**d**) Killing of shRNA transduced Tregs by HMEC-1 cells transduced with either GFP or FasL. Data are means ±SEM pooled from four independent experiments using unique healthy donors. *P* values determined by Student's t test. (**e**) Killing of T cells transduced with anti-apoptotic genes by HMEC-1 cells transduced with either GFP or FasL. Data are means ±SEM pooled from four independent experiments using unique healthy donors. *P* values determined by Student's t test. (**f**) Representative images of CD8 and Foxp3 cells in sections taken from subjects with ovarian cancer expressing either $FasL^+$ or $FasL^-$ vessels. Original magnification, 400×; scale bar, 50 μm. (**g**) Intratumoral CD8 T cell counts from human TMAs associated with percentage of $FasL^+$ vessels. High/low determinations based on median values. *P* values determined by Student's t test.

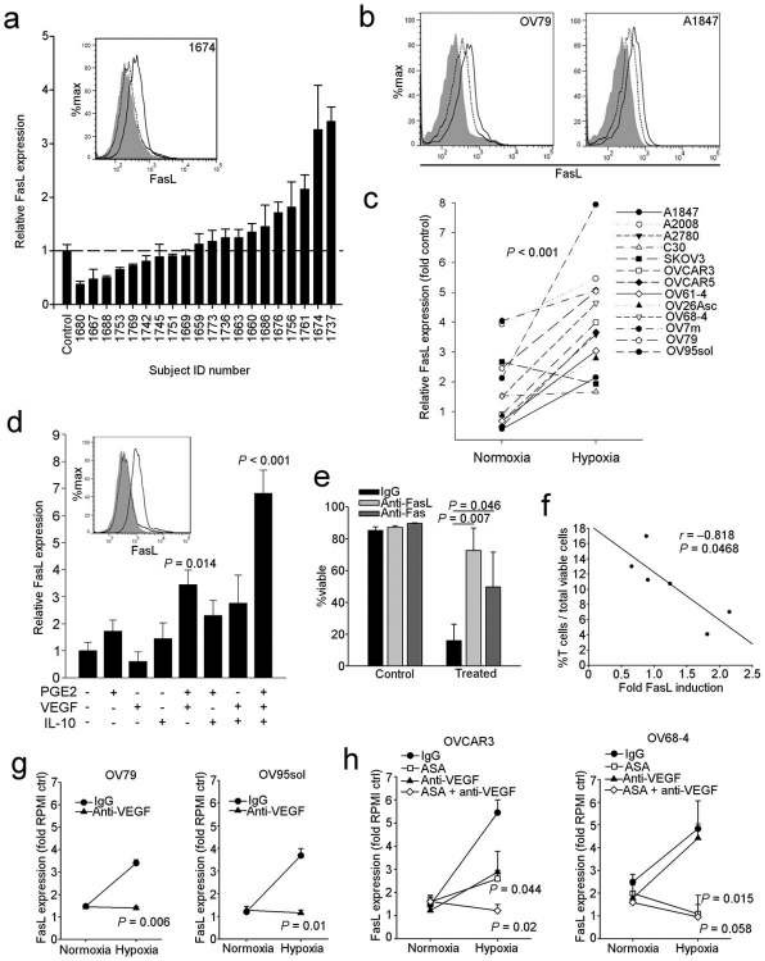

Figure 3. Expression of FasL by endothelial cells is regulated by the tumor microenvironment

(**a**) Ascites taken from individuals with ovarian cancer induces expression of FasL on HMVECs *in vitro*. Inset is sample flow cytometry of experiment. Shaded histogram is isotype control, dotted line histogram is RPMI media control and solid line histogram is FasL staining from a representative subject (#1674). Relative FasL expression was calculated as the median fluorescence intensity (MFI) of the isotype control subtracted from the MFI of treated cells divided by similarly subtracted MFI from RPMI control cells. Representative of two independent experiments. (**b**) Representative histograms of FasL induction on HMVECs by ovarian cancer cell line supernatants from the lines indicated. Shaded histogram is the RPMI media control, dotted line histogram is from cells treated with normoxic supernatant and solid line histogram is from cells treated with hypoxic supernatant. (**c**) Summary of ovarian cancer cell line supernatant treatments from three independent experiments. Data points are means of fold RPMI control calculated as in panel a. *P* value determined by paired Student's t test. (**d**) HMVECs treated with various combinations of cytokines. 1 μM PGE2, 50ng mL^{-1} VEGF-A, and 10ng mL^{-1} IL-10 was used. *P* values determined by one-way ANOVA followed by a Holm-Sidak post-hoc test. Inset is sample flow cytometry from the experiment. Shaded histogram is the isotype control, dotted line histogram is the untreated control and solid line histogram is from

HMVECs treated with all three factors for 24 h. Similar results were obtained with HUVEC and HMEC-1 cells (not shown). (**e**) Killing of Jurkat cells by HMVEC cells treated with 1 μM PGE2, 50ng mL^{-1} VEGF-A, and 10ng mL^{-1} IL-10 for 24 h. Data from three independent experiments. *P* values determined by Student's t test. (**f**) Negative correlation of the percentage of T cells, as assessed by flow cytometry, from enzyme-digested tumors, and the ability of subject-matched ascites to induce FasL *in vitro*. (**g**) Cell culture supernatants were used to treat HMVECs for 24 h as in panel c pretreated with anti-VEGF-A antibody or isotype control as indicated in the methods. Data from three independent experiments. (**h**) Cell culture supernatants from cells treated with 200 μM aspirin or vehicle were used to treat HMVECs for 24 h as in panel c pretreated with anti-VEGF-A antibody or isotype control as indicated in the methods. *P* values determined by Student's t test. In all panels, data are means ±SEM.

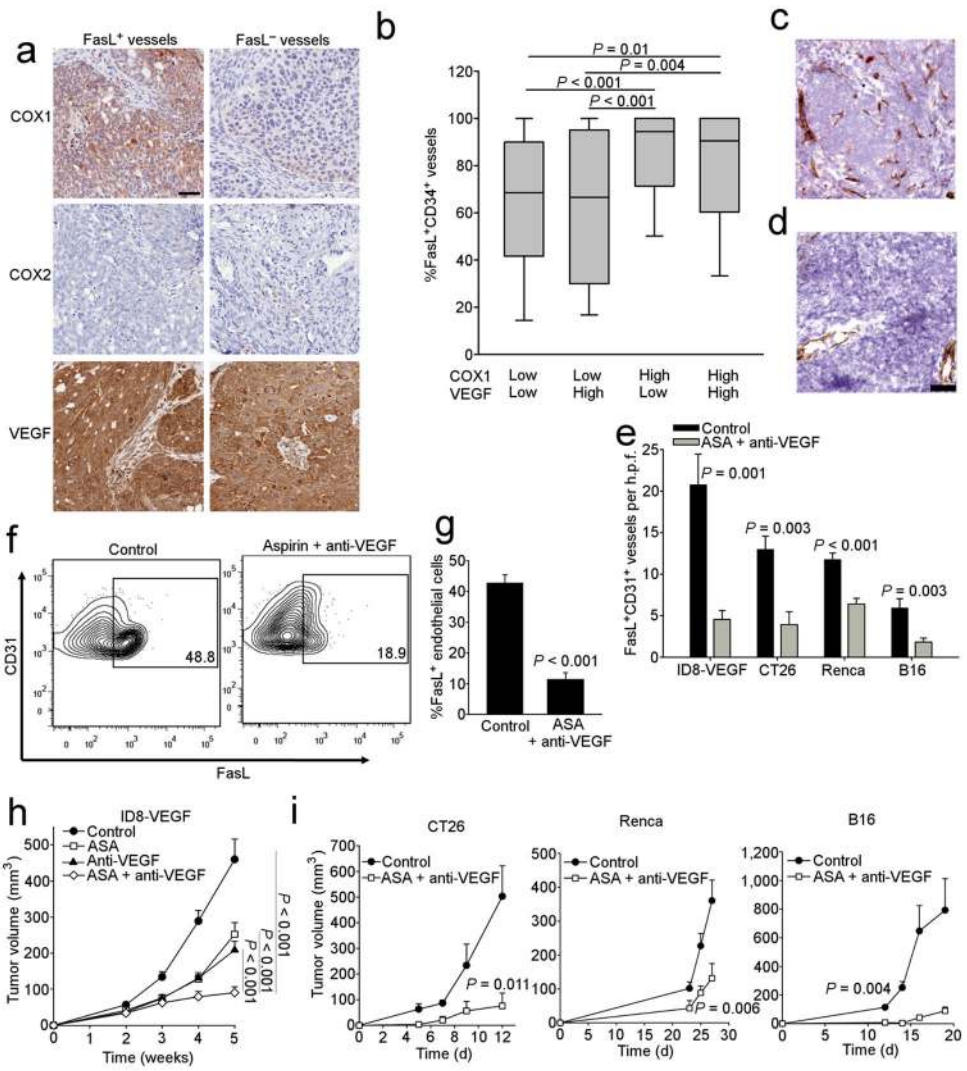

Figure 4. Proangiogenic growth factors induce FasL expression *in vivo*

(**a**) Expression of COX1, COX2, and VEGF-A in tumors from individuals that express either FasL$^+$ or FasL$^-$ vessels. Original magnification, 200×; scale bar, 50 μm. (**b**) Percentage of vessels from subjects with ovarian cancer that are FasL$^+$ divided by COX1 and VEGF-A expression based on a 0-3 score. Low/high determinations divided at the median. *$P < 0.05$ determined by Kruskal-Wallis followed by a Dunn's post-hoc test. Expression of FasL (red) on CD31 vessels (brown) in ID8-VEGF tumors from (**c**) control mice or (**d**) those treated with anti-VEGF-A and Aspirin for 5 wks as described in the methods. Original magnification, 200×; scale bar, 50 μm. (**e**) Quantification of FasL$^+$CD31$^+$ vessels determined by IHC from the indicated control tumors or those from mice treated as indicated. $n = 7–10$. P values determined by Student's t test, All data are means ±SEM. (**f**) Expression of FasL on CD45$^-$CD31$^+$ tumor endothelial cells in ID8-VEGF tumors from control mice or those treated with anti-VEGF-A and Aspirin for 5 wks as described in the methods. Gating determined by isotype control staining of CD45$^-$CD31$^+$ tumor endothelial cells. (**g**) Quantification of flow cytometry data from panel e ($n = 5$ per group). P values determined by Student's t test. All data are means ±SEM. (**h**) Growth curves of ID8-VEGF

tumors from mice treated as indicated. $n = 6–10$. P values determined by Student's t test. All data are means ±SEM. (**i**) Growth curves of indicated tumors from mice treated as indicated. $n = 7–10$. P values determined by Student's t test. All data are means ±SEM.

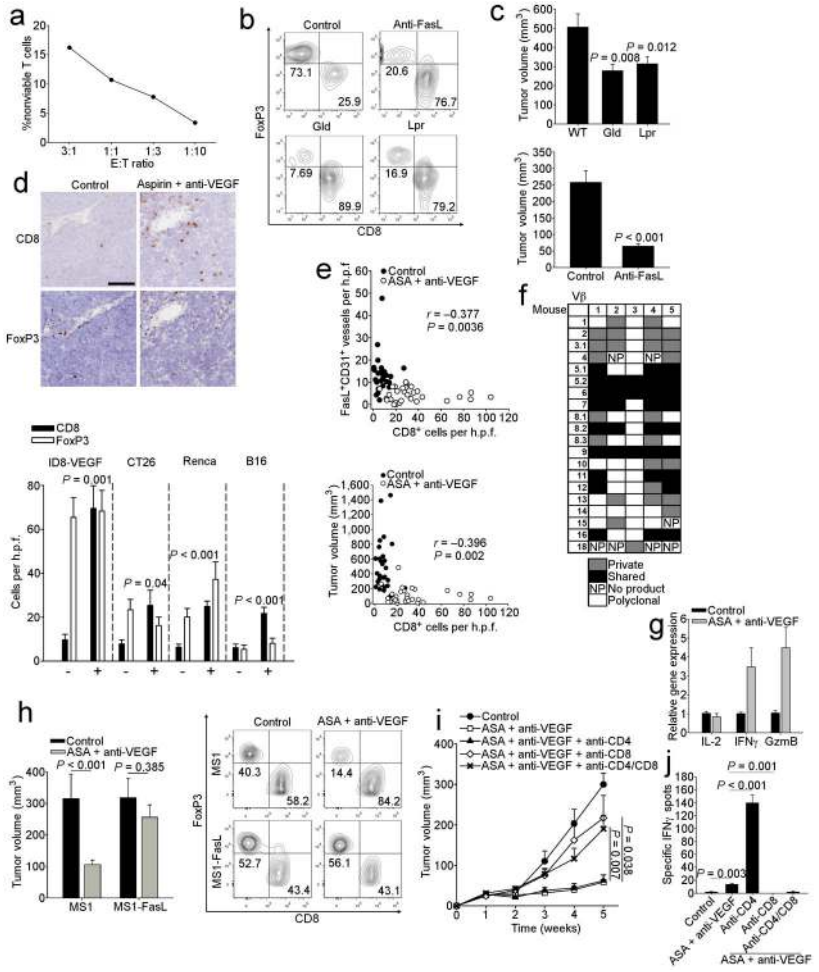

Figure 5. Endothelial FasL expression limits antitumor immunity by suppressing CD8 T cell infiltration in mice

(**a**) Viability of T cells following co-culture with endothelial cells isolated from ID8-VEGF tumors. Viability determined by flow cytometry using annexin-V staining following co-culture for 24 h. Shown is a representative experiment. (**b**) Flow plots of $CD3^+CD8^+$ T cells and $CD3^+CD4^+CD25^+Foxp3^+$ Treg cells (Boolean-gated, FoxP3 used as axis) isolated from 5 wk ID8-VEGF tumors grown on the indicated mouse genotype, control, or treated with anti-FasL antibody. (**c**) Tumor volumes from 5 wk ID8-VEGF tumors grown on the indicated mouse genotype or control. $n = 10–14$ per group. Also shown are tumor volumes from 4 wk ID8-VEGF tumors from mice injected with either anti-FasL or control IgG. $n = 5$ per group. *P* values determined by ANOVA followed by a post-hoc Dunn's test,and Student's t test, respectively. (**d**) IHC staining of 5 wk ID8-VEGF tumors grown on the indicated mice or treated with anti-VEGF-A antibody and aspirin. Original magnification, 200×; scale bar, 100 μm. Quantification of CD8 and FoxP3 IHC staining of the indicated tumors from mice treated with anti-VEGF and aspirin (+) or control (−). $n = 7–10$ per group. *P* values determined by Student's t test. All comparisons shown are for CD8 cells as no significant differences were observed between controls and treated mice for FoxP3. (**e**) Pooled correlations of indicated parameters from mice bearing ID8-VEGF, CT26, Renca,

and B16-LU8 tumors. *n* = 58. *P* values determined by Pearson's test. (**f**) Spectratype analysis of TCR Vβ chains in ID8-VEGF tumor bearing mice treated with aspirin and anti-VEGF-A for 5 wks. (**g**) Expression of IL-2, IFN-γ and granzyme B by qRT-PCR. Data are pooled from two independent experiments, *n* = 6 per group. (**h**) ID8-VEGF tumor volumes at 5 wks of mice injected with either control MS1 or MS1-FasL endothelial cells. *n* = 5 per group. *P* values determined by Student's t test. Flow plots of $CD3^+CD8^+$ T cells and $CD3^+CD4^+CD25^+Foxp3^+$ Treg cells (Boolean-gated, FoxP3 used as axis) isolated from corresponding tumors. (**i**) Growth of ID8-VEGF tumors in mice treated with aspirin and anti-VEGF-A for 5 wks and depleted of the indicated T cell subset. *n* = 8. *P* values determined by Student's t test. (**j**) ELISpot from mice in panel h at 5 wks using ID8-VEGF cells as targets. *P* values determined by Student's t test. In all panels, data are means ±SEM.

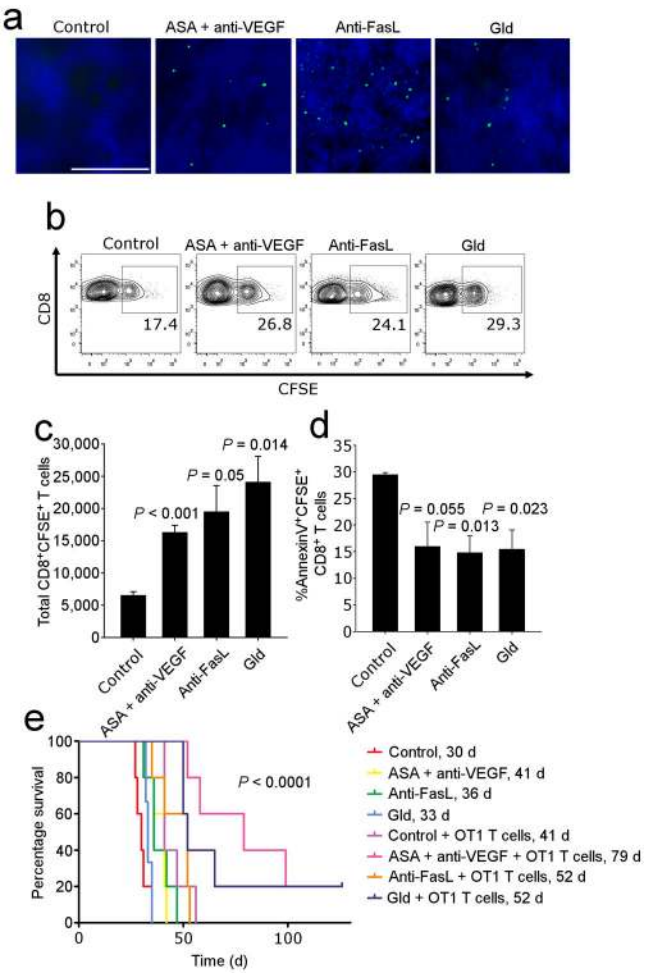

Figure 6. FasL blockade enhances T cell infiltration

(**a**) Infiltration of CFSE labeled T cells. Original magnification, 400×. Scale bar, 100 μm. (**b**) Detection of CFSE labeled cells by flow cytometry. Gated on $CD8^+$ T cells. (**c**) Quantification of $CFSE^+$ cells in the tumor. Data are means ±SEM. *P* values determined by ANOVA followed by post-hoc Holm-Sidak test. (**d**) Viability of $CFSE^+CD8^+$ T cells determined by AnnexinV staining. $n = 5$ per group. Data are means ±SEM. *P* values determined by ANOVA followed by a post-hoc Holm-Sidak test. (**e**) Survival following adoptive transfer of OT-1 cells into i.p. ID8-VEGF OVA tumor-bearing mice. $n = 5$ per group. Data are representative of two independent biological experiments. *P* value determined by the Log-Rank test.